Assessment of tropical cyclone-induced shoreline and riverbank changes at the Rufiji Delta using satellite remote sensing methods

Kombo H. Kai [1]*, Julius Francis [2], Yohanna W. Shaghude [3]

[1] Tanzania Meteorological Authority (TMA), PO Box 340, Zanzibar

[2] Western Indian Ocean Marine Sciences Association (WIOMSA), PO Box 3298, Zanzibar

[3] Institute of Marine Sciences (IMS), PO Box 668, Zanzibar

* Corresponding author:
kombokai68@gmail.com

Abstract

The study aimed at quantifying changes in shoreline and the riverbanks caused by tropical cyclones (TCs) and associated rainfall in the Rufiji Delta, southern Tanzania. Long term changes of the shoreline and riverbanks were analysed using medium resolution (Landsat TM and ETM) satellite imagery (1991, 1997 and 2007), while short-term changes (2013 to 2014) were analysed using high resolution (Pleiades) satellite imagery. Delineation of the shoreline and riverbank changes were accomplished through the analysis of appropriate coloured image composites, Sobel filtering and maximum likelihood classification of land cover. Analysis of Landsat data showed a relatively higher magnitude of erosion between 1991 and 2007, followed by minor changes between 1997 and 2007. Simbauranga was the most severely eroding site, with an estimated magnitude of erosion of 83 to 100 m during the study period. The maximum magnitude of short-term changes of the riverbanks were estimated at about 31m². Apart from the erosion of the riverbanks, other changes were the conversion of water to vegetation covered areas (amounting to approximately 200 m²). Short-term shoreline changes were up to 206 m with higher magnitude of accretion (142 m) than erosion (-4 m). The study conclusively calls for detailed research on shoreline and riverbank changes based on the impacts of TCs on land cover.

Keywords: shoreline and riverbanks, erosion and accretion, maximum likelihood classification, band combinations, Sobel filtering

Introduction

Tropical cyclones (TCs) are low pressure systems that form over warm tropical waters with gale force winds of at least 17.5 ms⁻¹ and gusts exceeding 25 ms⁻¹ near the centre (Holland, 1993). They are non-frontal low-pressure systems of synoptic scale having organized convection and a life span of at least six hours (Bengtsson, 2007). Actual wind speeds recorded from South Western Indian Ocean (SWIO) TCs include 70 ms⁻¹ for Bondo (December, 2006) and 69 ms⁻¹ for Hurry (March, 2012).

TCs have adverse impacts on society and their socio-economic well beings. Among the most common adverse impacts of TCs include the destruction of settlements and assets, public infrastructure (such as roads, telecommunication lines, schools, etc.) and crops (Charrua *et al.*, 2021). Such impacts are often caused by strong winds which are accompanied by heavy rains during the TCs and storm events. The extent of damage is often influenced by the coastal geomorphology, the nearshore ocean topography, the TC/storm track and the vertical changes in atmospheric pressure (Camargo *et al.* 2013; Yanxia *et al.*, 2013). Moreover, the associated coastal flooding (inundation) and the huge waves or swells which accompanied the TCs are considered to be the main cause of damage to coastal human settlements and public infrastructure (Chang-Seng and Jury, 2010).

Apart from the socio-economic impacts, TCs are also associated with considerable environmental impacts which include coastal erosion and redistribution of nearshore and offshore sediments (Nyandwi, 2001; Lacombe and Cater, 2004; Cooper *et al.*, 2008), which may in turn adversely affect nearshore habitats such as coral reefs.

The problem of shoreline changes, particularly coastal erosion, is considered to be one of the major environmental management issues in Tanzania and most parts of the Western Indian Ocean Region (Shaghude *et al.*, 2007; Shaghude *et al.*, 2015). Although a wide range of studies have been undertaken to establish the magni-

short-term shoreline and riverbank changes associated with TC events.

Materials and methods
Study area

The Rufiji Delta which is located along the southern coast of Tanzania has the largest mangrove forest cover in East Africa (Semesi, 1992). The mangrove forests fall within the protected forest reserves of Tanzania. One of the unique features of the mangrove forest reserve of the Rufiji Delta is that there are legally established village settlements (with an estimate of about 49,000 people (Mangora et al 2018) exists within it. These people depend on mangroves and the associated marine
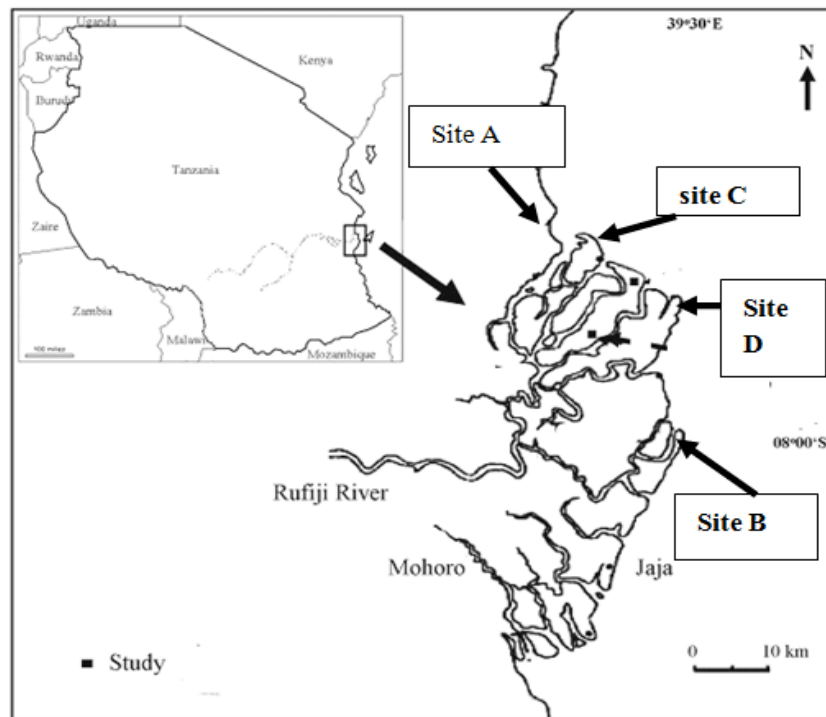
Figure 1. Study area location in the Rufiji Delta indicating of the four study sites (A to D). Modified after Punwong (2013).

tude of erosion at different locations, and identifying the main causative factors and impacts along the coast (Shaghude *et al.*, 2003; Muzuka, 2001; Muzuka and Shaghude, 2000; Shaghude, 2004; Shaghude *et al.*, 2015), no study has yet quantified the magnitude of shoreline or riverbank erosion associated with TCs along the Tanzanian coast. Thus, the main objective of this study was to describe and assess the impact of severe weather events such as TCs and the associated heavy rainfall on shoreline and riverbank changes in the Rufiji River using satellite remote sensing data (1991, 1997 and 2007). Specifically, the focus of the study was to examine and to quantify the long- and

environment for a range of resources and ecosystem services to support their livelihoods. According to Monga *et al.* (2018) the local communities who live in and around the Delta are directly engaged in various socio-economic activities such as rice farming, cutting of mangrove poles and timber, and fisheries.

The Rufiji Delta is approximately 65 km wide and extends for about 123 km inland (Semesi, 1992; Erftemeijert and Hamerlynck, 2005; Punwong, 2013). Within the Delta system, the Rufiji River branches into a series of distributary channels, including the Bomba, Kikale, Kyomboni, Mchingamfisini amongst

others. The Delta is broadly divided into two mor-phological units, the southern and northern Deltas, which extend for about 23 km along a north-south direction and with an east-western extent of about 70 km (Doody and Hamerlynck, 2003). The Delta man-groves substrata forms the dominant component of the Delta substrates, while sand beaches and intertidal sand flats occur as subordinate substrates on the Delta. The mangrove substrata occur at approximately 2.5 m above mean sea level (Fisher *et al.*, 1994; Fisher and Overton, 1994).

The tides on the Delta are semi-diurnal with a tidal range varying from 2-2.5 m to about 3.3 - 4.3 m dur-ing high spring tides (Fisher *et al.*, 1994; Richmond *et al.*, 2002: Francis, 1992). The water and soil salinity along the Delta ranges from 10.60 ‰ to 32 ‰ (Francis, 1992; Fisher *et al.*, 1994), while observations show that the water in pools in non-mangrove covered areas can have a salinity as high as 85 ‰.

Inland, the Rufiji River is linked to three tributaries which drain the Upper Rufiji catchment. These three tributaries; the Luwegu, Kilombero and Great Ruaha Rivers, supply 18 %, 62 % and 15 % of the total inflow to the Rufiji River, respectively (Hufslund, 1980; RUBADA, 2001; Shaghude, 2016). Moving from the Delta towards the hinterland, the climate varies with the topography, with the Delta coastal areas, which are located at the lowest elevations, being characterized by high temperatures (24-28 °C) (Timiza, 2011; Nde-sanjo *et al.*, 2012) and lowest annual rainfalls (700 mm) (FAO, 1960). By contrast, the areas over the Upper Rufiji catchment, located at 100-200 m above sea level are characterized by relatively lower air temper-atures (between 23 °C and 28 °C) and higher precip-itation (over 1000 mm per year). Both the Delta and the areas located over the Upper Rufiji catchment are geographically located in areas that are characterized by a unimodal rainfall pattern (Timiza, 2011) with the rainy season occurring from December to March (DJFM). The DJFM rainy season is also the peak time for TCs in the SWIO basin (Kai, 2018). The season is also characterized by frequent storms (Mavume *et al.*, 2006) and heavy rainfalls, which in turn generate huge volumes of water in the river drainage systems that is also associated with coastal inundations and river bank erosion (Kai, 2018; Kai *et al.*, 2021).

Data
Satellite data
The data used for this study consisted of: 1- Medium resolution (30 m by 30 m) Landsat satellite imagery from May, 1991, July, 1997 and June, 2007 (path 166, row 65 and 66) acquired from the Global Land Cover Facilities (GLCF; http:// landcover.org/); and 2- High resolution Pleiades satellite imagery covering an area of about 7 x 8 km² with a spatial resolution of 0.5 m x 0.5 m (panchromatic sensor) and 2 x 2 m (multispectral sensors). The satellite imagery was used to determine the historical shoreline positions at the Rufiji Delta using a cost-effective change detection technique (Lohani and Mason, 1999). In particular, the Landsat imagery from May, 1991, July, 1997 and June, 2007 were used to assess long term shoreline changes over the Delta, while the high-resolution Pleiades imagery was used to assess the short-term riverbank erosion/ accretion changes along the Rufiji Delta and its dis-tributary channels. The acquisition dates of the three Landsat images were targeted to tie with the Decem-ber to May rainfall season and peak TC period over the SWIO basin. An attempt was made to assess the importance of episodic shoreline changes occurring during the periods characterized by strong El Nino events (such as the 1997/1998 El Nino) and uniform rates of shoreline changes influenced by weak El Nino events. In this study, the images which was considered to qualify for the assessment of shoreline changes were those which were almost cloud free (at least 94 % cloud free) over the study area. As for short-term pre- and post-storm shoreline and riverbank changes, images from the 2013/2014 TC season were used to capture the entire DJFM period. The pre- and post-storm image acquisition dates for six storms during the 2013/2014 TC season are as shown in Table 1.

Tidal data/Tables
Tides influence the shoreline dynamics through the daily rise and fall of the sea water under the influence of the gravitational forces of the moon and to a lesser

Table 1. Pre- and post-storm images captured. Names and dates for six cyclones from December 2013 to March 2014.

Images captured		Storms (name and dates)					
Pre-storm	13/09/2013	Amara	Bruce	Collin	Besija	Fobane	Hellen
Post-storm	13/06/2014	14/12/2013	19/12/2013	09/01/2014	28/12/2013	6/02/2014	27/03/2014
		23/12/2013	24/12 2013	15/01/2014	06/01/2014	14/02/2014	01/04 2014

extent also the sun (Williams and Thom, 2001; Williams *et al.*, 2003; Yanxia *et al.*, 2013). Thus, to eliminate the tidal influence on the assessment of shoreline changes due to TC events, it was important to use the images acquired during low tides of the daily tidal cycle (Pugh, 1996; Nyandwi, 2000; Nayak, 2002). As there was no tide information specifically for the Rufiji Delta, the study used the information for Dar es Salaam and Mtwara to estimate the time for the occurrence of low water at the Rufiji Delta which is geographically located approximately mid-way between Dar and Mtwara. The tide tables for Dar es Salaam and Mtwara were downloaded from http://tides.mobilegeographics.com/ locations/1490.html and http://tides.mobilegeographics.com/locations/3949.html, respectively. Furthermore, all images used in this study were preferably acquired at approximately the same low tide levels as recommended by other studies (Nyandwi, 2000; Nayak, 2002; Pugh; 2004; Shaghude, 2003, 2004; Boak and Turner, 2005). For short-term shoreline changes, the images were selected by taking into consideration that the key factors contributing to shoreline changes during the pre- and post-storm events are comparable. Moreover, during the field trips, Ground Control Points (GCPs) at specific monitoring sites (areas considered to be experiencing considerable changes as evidenced from digital image analyses of the satellite remotely sensed data) were taken and used for subsequent validation (geometrical rectification) of the remotely- sensed data.

Methods

The Landsat images were geo-referenced using the Arc map 10.2.2 (toolbar for projection) and WGS 1984 Zone 37°S Universal Transverse Mercator (UTM) coordinate system, which corresponds to the location of the eastern parts of Tanzania. During processing of the Landsat images, the atmospheric correction was not taken into consideration because the difference in shorelines between the two dates was determined by image differencing, which does not necessitate the atmospheric correction (Singh, 1989). The de-striping

algorithm developed by USGS (Tsai and Chen, 2008) was used to remove the stripes for the Landsat 2007 image. Furthermore, atmospheric correction was not performed for Pleaders images because (i) the temporal variability of the selected images were within the same season, and (ii) the algorithm used for determining change detection used training data from the same location and same season and no multiple seasons or places were used (Singh, 1989; Song *et al.*, 2011; Chinsu *et al.*, 2015).

Analysis of shoreline changes (delineation) was carried out in two main steps; namely 1- Visual analysis of the images using colour composite images, and 2- digital image classification (Pardo-Pascual *et al.*, 2012; Dolan *et al.*, 1980). The visual analysis of the imagery was undertaken using Arc map 10.2.2 and GRASS software. Considerable contrast between water and land was clearly evident especially when the near infrared (NIR) and mid infrared (MIR) bands were used, as noted by Jensen (1996).

To get the best contrast between water and sand, the three bands 7 (Red), 5 (Green) and 4 (Blue) false colour composites were used. The three bands combination provided the best atmospheric penetration of the electromagnetic radiations, where the coastlines and shores became clearly delineated. The other alternative band combinations of 7 (Red), 5 (Green), and 3 (Blue) false colour composites also provided clearly delineated coastlines and water features within the image.

Classification of various types of land cover was accomplished using supervised digital imagery classification with maximum likelihood algorithms and two classes (i.e., water and land for the Landsat imageries) and five classes, (i.e., land, vegetation, grass, shallow water and deep water for the Pleiades imageries). During the maximum likelihood classification, Google Earth Imagery for the Rufiji Delta site was used to identify training signatures for water, sand (bare land), vegetation and grass land cover features.

Table 2. Description of the images and tidal records for both shoreline changes over short- and long-term settings. Note that the Pleiades images consisted of 4 bands (Bands 1 to 4), with spatial resolution of 2 x 2 m for the multispectral bands, and 0.5 x 0.5 m for the panchromatic band. The mean tidal height between Dar es Salaam and Mtwara was used to estimate the tidal height at the Rufiji Delta data.

No	Scene Sensor	acquisition date	Scene central time	Tidal height f for Dar (m)	Tidal height for Mtwara (m)
1	TM5	29/05/1991	07:20:55.5130750Z	0.2	0.8
2	TM5	16/07/1997	07:02:55.5130750Z	1.5	2.0
3	ETM7	18/06/2007	07:22:40.8780071Z	1.2	1.0
4	Pleiades	17/09/2013	12:56:11Z	2.8	3.0

Analysis of the high-resolution Pleiades imagery followed similar protocols, where the training classes were; shallow water, sand (bare land), deep water, vegetation, grasses (as defined from the Google Earth imagery through visual analysis). The Arc map (10.2.2) toolbar for measuring areas and lengths was used to measure the deviation of the extracted shoreline from the reference shoreline. Distances measured to the right of the reference shoreline (i.e., towards the water) were conventionally considered as positive (i.e., accretion of the shore) and those measured to the left of the reference shoreline (i.e., towards the land) were considered as negative (signifying erosion of the shore). The perpendicular distances between two corresponding points of the two historical shorelines were measured to determine the overall direction of change (mean accretion or erosion). The net magnitude of erosion and accretion was then determined. Lastly, the shoreline shape files were compared with the reference coastline to assess the level of precision of the digitizing method.

Results and discussion

The results showing riverbank changes during 1991 – 1997 and 1997 – 2007 are presented in Fig. 2. The results indicate that considerable riverbank changes occurred from 1991 - 1997 as compared to 1997-2007. The results further show considerable sediment accretion taking place along the Rufiji Delta distributary channels, during some of the flooding events (Fig. 2b). The highly pronounced bank accretion along the Rufiji Delta distributary channels could be attributed to the super El Nino event of 1997-1998. The distributary channel

bank accretion observed in 1997/1998 are in marked contrast to the bank erosion that is clearly observable in 1991 (Fig. 2a). The results further revealed that the two periods (1991-1997 and 1997-2007) were characterized by a sequential decrease in vegetation cover over the Delta; a phenomenon which may explain the observed accelerated erosion/sedimentation pattern (Fig. 3 and 4).
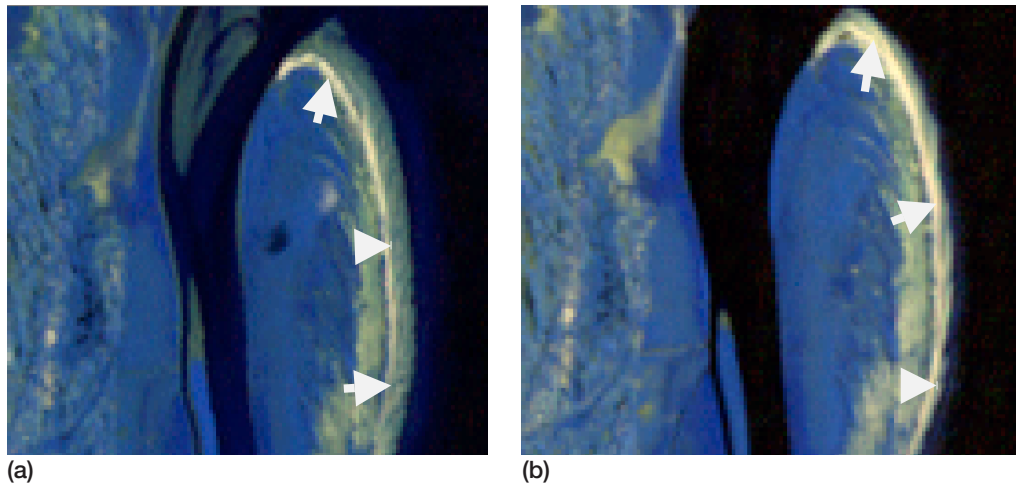
The observed shoreline changes along the Rufiji Delta for the period 1991 - 1997 are presented in Fig. 3. The results show that considerable accretion of the shoreline occurred during the period 1991 - 1997, especially in the northern parts of the Delta (Fig. 3b). The observed changes are illustrated by the observed differences of the shoreline width between the 1991 and 1997 satellite imagery. Very few changes along the shoreline were observed during 1991 – 2007. However, considerable reduction of shoreline width during 1997 to 2007 was evident (Fig. 4).

Analysis of the magnitude of shoreline accretion at the four sites near the river mouth (Fig. 1) show different levels of shoreline accretion along the Rufiji River mouth (Table 3). Highest magnitude of shoreline changes during the cited periods (1991 to 1997, 1997 to 2007, 1991 to 2007) were are generally observed at sites A and B respectively, and relatively lower magnitudes of shoreline changes were observed at the remaining sites.

The results further revealed that shoreline digitization using both manual (band combinations) and automatic

(a)   (b)
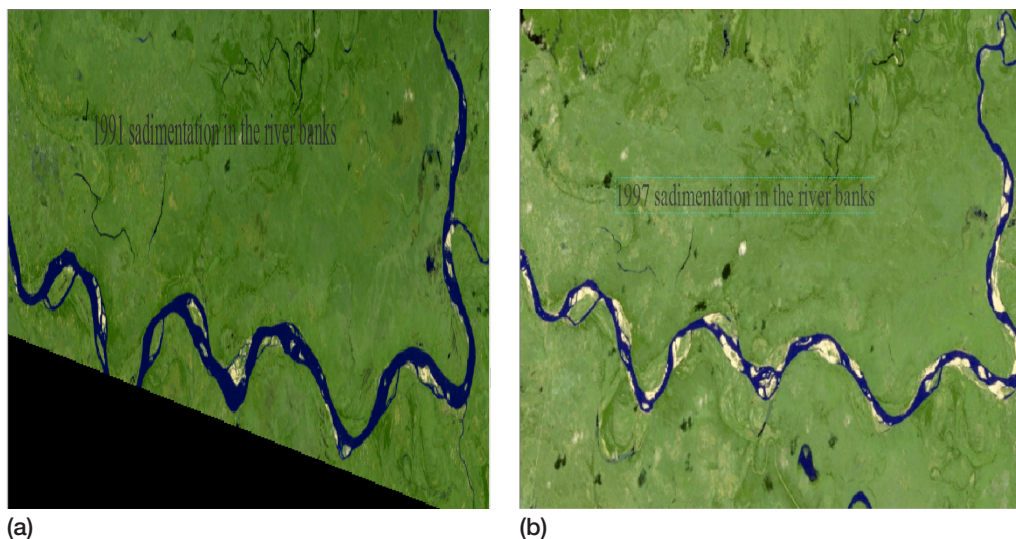
Figure 2. Variation of sediments in upstream meanders of selected parts of the Rufiji Delta distributary channel for the years 1991(a) and 1997(b). The white patches along the river bank shows the sand /sediment depositions. .

Figure 3. Observed shoreline changes along the Rufiji Delta during 1991(a) and 1997(b), as deduced by the false colour composite imagery represented by bands 7, 5 and 4 (Red, Green and Blue, respectively). The white arrows indicate the areas of signifcant shoreline changes from 1991-1997.

(supervised maximum likelihood classification) had comparable results. Moreover, the results revealed that 1997 was the period of highest shoreline erosion in the Rufiji Delta, while in 1991 there was considerable shoreline accretion due to deposition of sediments into the shoreline. The observed higher magnitudes of erosion could be explained by the strong El Nino event which is contrasted with the weak 2007 El Niño event, where considerable accretion of the riverbanks were observed. Furthermore, the results in Fig. 3 (a - b) revealed sequential erosion at Site A and Site C (Simbauranga) from 1991 to 2007, while Fig. 3 (c - d) shows that the erosion and accretion rates were altering from year to year at Site D and Site B.

The results presented in Table 3 were consistent with the observations deduced from the Google Earth satellite image of June, 2007 (Fig. not shown here) which also revealed that Site C (Simbauranga) had been consistently experiencing erosion throughout the three time periods; i.e., 1991 - 1997, 1997 - 2007 and 1991 - 2007.

The analysed images on riverbank erosion and accretion revealed that, while some parts displayed accretion at a magnitude of about 7 m², others had even higher magnitudes of accretion, reaching up to between 26 m² and 31m² (Fig. 5, 6). The results presented in Fig. 5 (a and b) show that during the 2013/2014 TC and heavy rainfall season, an area of about 0.2 km² which was previously under water was converted to a mangrove forest. This could be due to the sporadic sedimentation that took place under the influence of cyclonic or storm events. Generally, the results showed that the observed erosion and sedimentation on the riverbanks had direct linkages with the waves and storms that were accompanied by the heavy rainfall events (Fig. 6); where the magnitude of erosion and accretion of riverbanks ranged between 26 m² and 31 m².

Analyses of shoreline changes using various image classification methods based on high resolution data sets (Pleiaders images) for pre- and post-storm conditions at three selected sites in the Rufiji Delta are presented in Table 4. Maximum likelihood classification

Table 3. Magnitude of shoreline changes, including accretion (AC) or erosion (ER) at four selected sites along the Rufiji River Mouth of the Rufiji Delta during the three time periods (1991, 1997 and 2007). ER and AC indicate average magnitude of erosion and accretion, respectively, while NTC indicates the direction of the net change. At Simbauranga (Site C) (1997 - 2007) and Site D (1991-2007) the changes were both negative (erosion) and positive (accretion) and tended to cancel each other out.

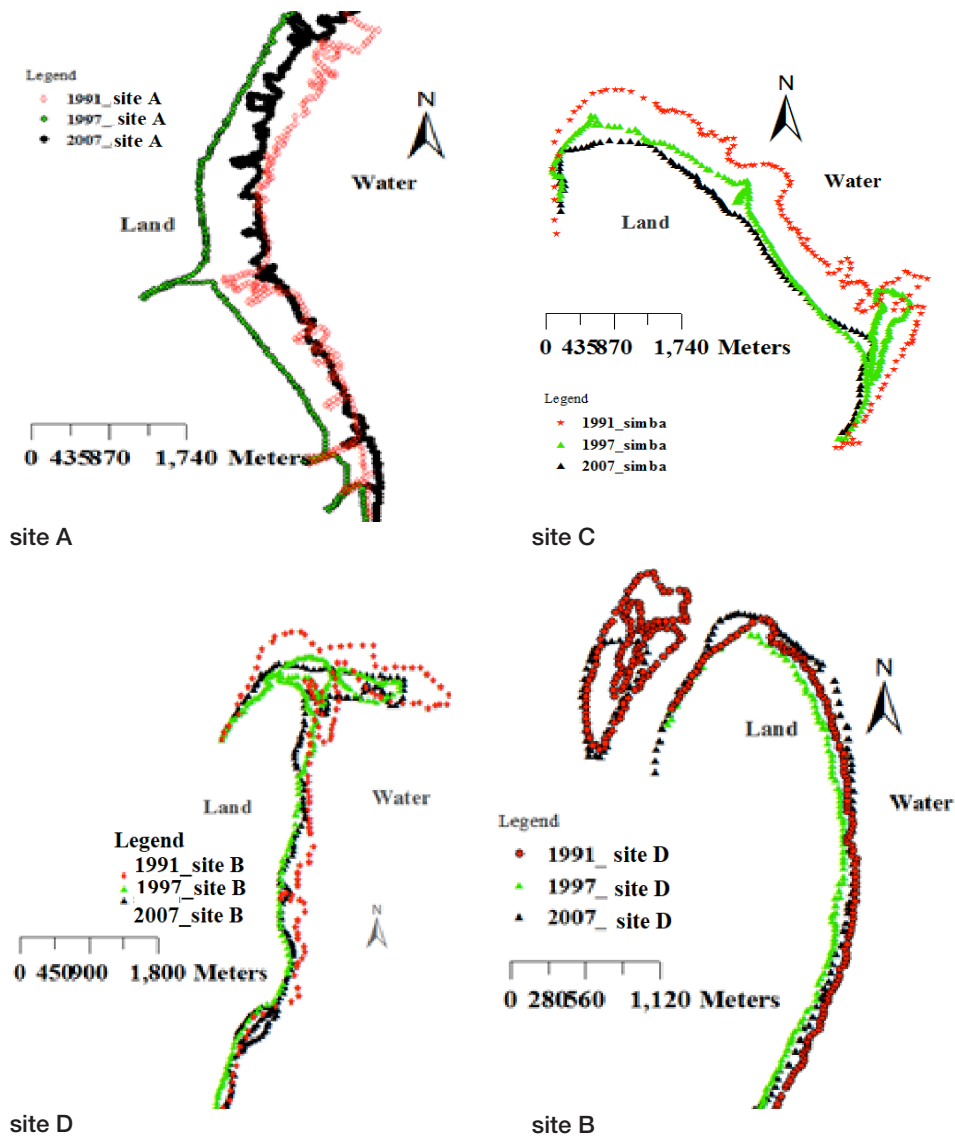| Years	Site A			Site B			Site D			Site C		
	ER	AC	NTC	ER	AC	NTC	ER	AC	NTC	ER	AC	NTC
1991-1997	25.7 - 100	0 - 15	ER	14.3-64.3	6.4-21.7	ER	0 -18.3	0	ER	0-94.6	0-1	ER
1997-2007	0- 2	11.6 - 83	ER	5.6-18	2 - 29.9	ER	0	3.9 - 21.8	AC	0 -28	0-19.5	ER & AC
1991-2007	7.6 - 38	4.7 - 29.2	AC	3.8 - 35.6	6.73 - 18.7	ER	0 - 10.5	0 - 11	ER & AC	2.8- 48	0	ER

Figure 4. Manually digitized shorelines for different shoreline areas of the Rufiji Delta using the maximum likelihood classification with two classes of Land and Water. The red curve indicates the 1991 shoreline changes, the blue curve indicates the 1997 shoreline and the black curve indicates the 2007 shoreline changes at different sites near the mouth of the Rufiji River as shown in Fig. 1.

and false colour composite classification methods provided slightly different results, with the false colour composite method giving lower values for both the magnitude of accretion and overall change. Furthermore, Sobel filtering using band 4 (NIR) seemed to work better than the band combinations and the maximum likelihood classification methods for delineating the shoreline. This could be explained by the fact that the problem of shallow water radiances and water turbidity was solved in Sobel filtering after merging land and vegetation with high reflectance in band 4 into one class. Moreover, composite analysis of the imagery using bands 4, 3 and 2, or bands 3, 2 and 1 could not solve the shallow water and water turbidity problem.

Furthermore, the presented results show that the maximum likelihood classification was a better land cover classifier than the band combination classification methods. The results of the former method (maximum likelihood classification) consistently agreed with the visual analyses of the Google Earth satellite images, while the results of the later method were highly inconsistent from one another, and with the visual analyses of the Google Earth satellite images. This could be explained by the fact that the method lacks the ability to distinguish wet sands and turbid water (i.e., when the level of inorganic materials in turbid water increases the water looks like the wet sand). The problem of shallow water and water turbidity radiances could be solved by using change
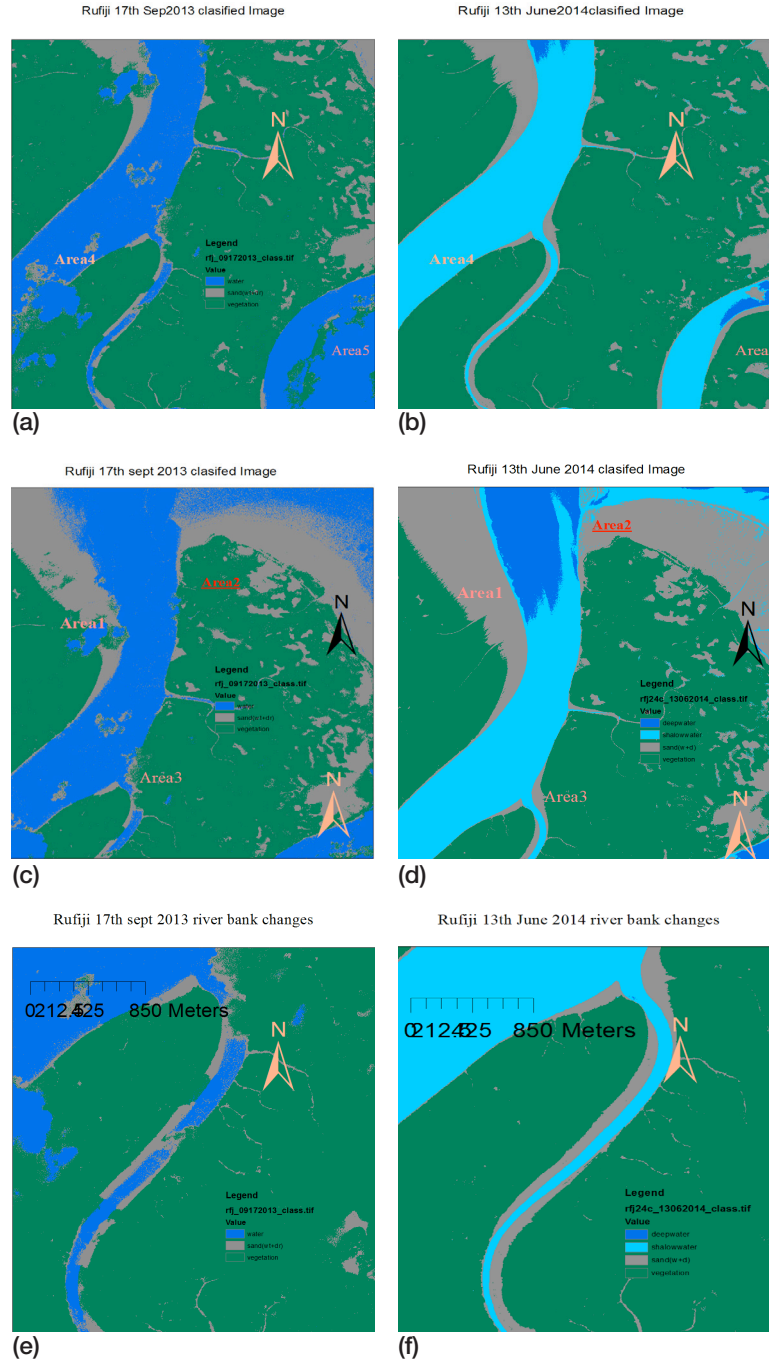
Figure 5. Sediment deposition and erosion along the Rufiji riverbanks as deduced from the classified images for the pre- (images on the left) and post- (images on the right) TC events, with areas covered by water (blue), sand (grey), and land (green). Images (a) and (b) show areas covered with water in pre-storm conditions, and covered with vegetation in post-storm conditions. Images (c) and (d) show three areas (Area 1, Area 2, and Area 3) with erosion in pre-storm conditions but sediment deposition in post storm conditions. Images (e) and (f) show extensive erosion in the river tributary in pre-storm conditions, but sediment deposition during post-storm conditions.

detection, employing subtraction between band 4 and band 3, or band 4 and band 2, or band rationing as discussed by Jensen (1996), Frouin *et al.* (1996) and Lohani and Mason, (1999). In this study these processes were not taken into consideration.

Additionally, the results presented on the magnitude of changes due to the influence of all cyclones over the given period, using three methods over the Rufiji Delta (Table 4) show that all the three methods showed relatively higher rates of accretion compared to erosion at
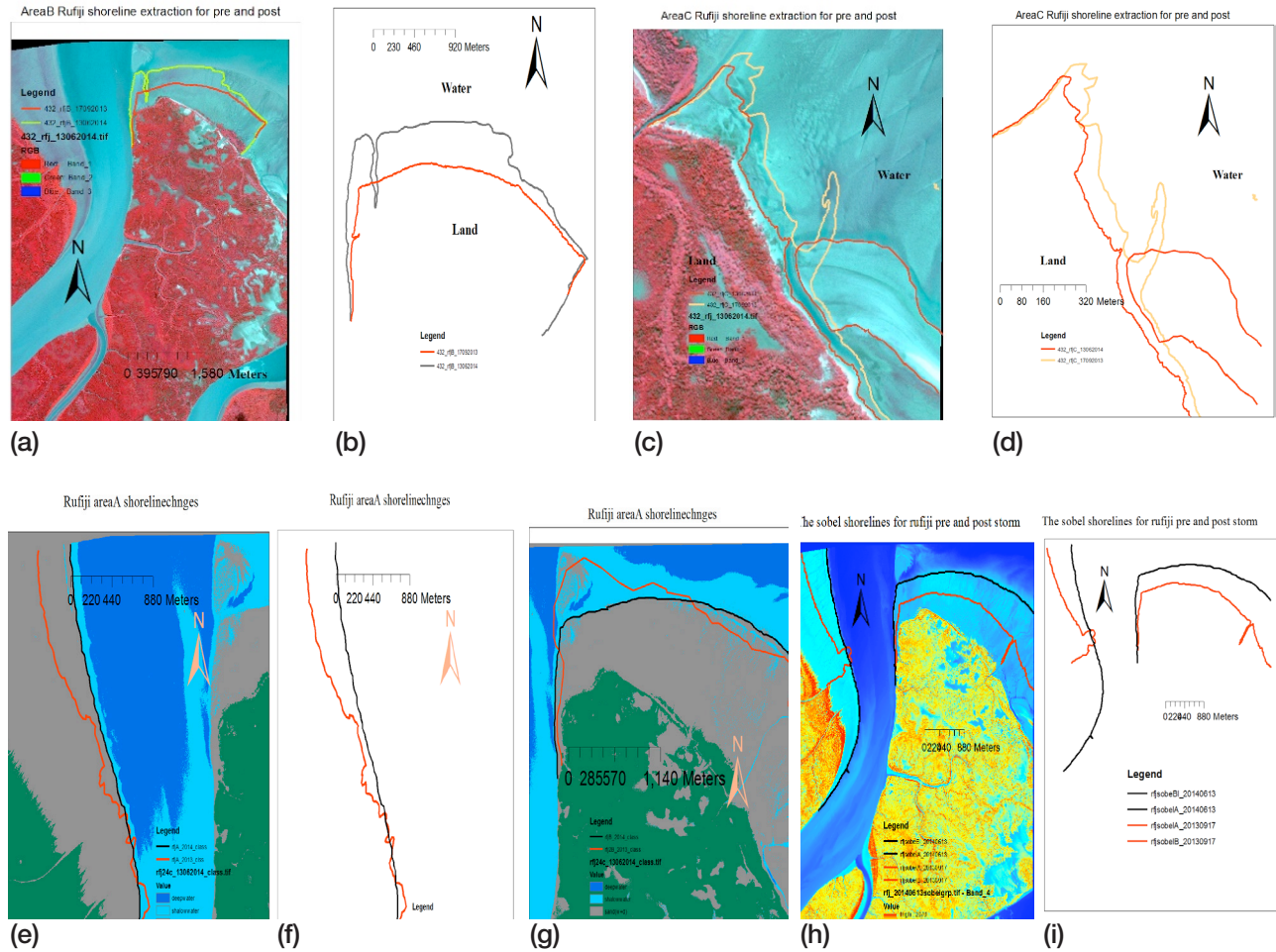
Figure 6. Digitized shorelines over the Rufiji delta using the true and false coluor composites (6a6d), maximum likelihood classification (6eand-6g) and Sobel filtering (6h and 6i) for pre- and post-cyclone conditions.

Site A. The Sobel filter method gave the highest magnitude of accretion (up to 393 m) followed by band combination (up to 244 m), and maximum likelihood classification gave the lowest magnitude of accretion (about 206 m). Moreover, all the three methods indicated that Site A had a relatively low magnitude of erosion, or no erosion at all. With the maximum likelihood classification (Fig. 6) Site C (Simbauranga) had the highest magnitude of erosion (of up to - 242 m) while the band combination and Sobel filter showed that this Site was not eroding and instead had been

accreting. In general, the Sobel filter and band combinations classification methods were found to be good delineators for the accretion process while maximum likelihood classification seemed to be a good delineator for both accretion and erosion processes.

Further assessment of the three classification methods was made by digitizing the shoreline changes at Site C (Simbauranga) pre- and post-storm events as observed during the field trips to the Rufiji Delta (Fig. 7). The results showed that despite the apparent differences

Table 4. Results of the computation of the magnitude of erosion/accretion (in meters and not m²) using maximum likelihood classification method, false colour composites, and Sobel filtering for the three selected sites in the Rufiji Delta.

Classification method	Maximum likelihood classification			False colour composite			Nonlinear egde enhancement (sobel)		
Type of change	Overall change	Accretion	Erosion	Overall change	Accretion	Erosion	Overall change	Accretion	Erosion
Site A	206	142	-42	244	244	-	393	393	-
Site B	-	-	-	37	52	-8.1	-	-	-
Site C	-8.7	100	-242	177	177	-	215	215	-
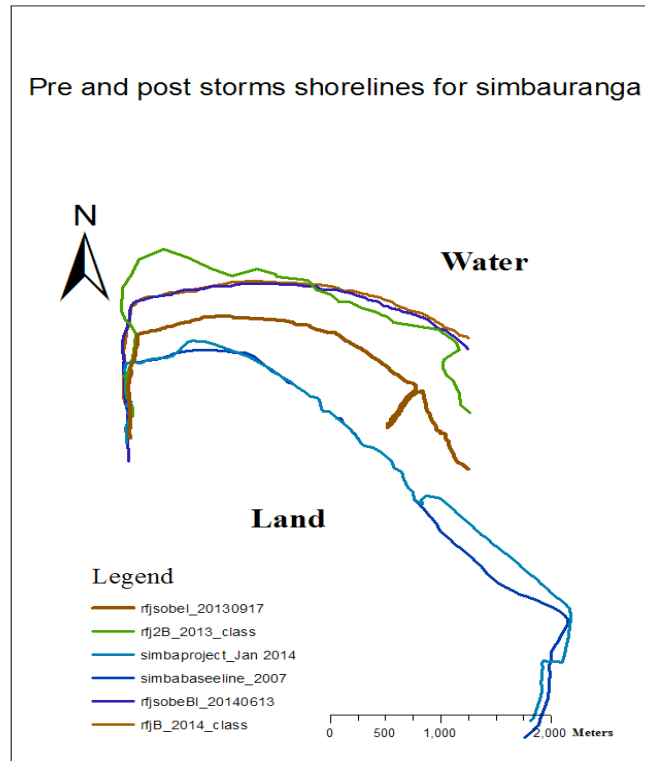
Figure 7. Digitized shorelines for Simbauranga pre- and post-storms of 2013/014, 2007 and the field survey of October, 2014.

between the three classification methods, all three methods revealed that Site A and Site C (Simbauranga) in the Rufiji Delta had been accreting over time.

Past studies had revealed that TCs along the coast of Tanzania mostly occur from December to May (Kai, 2018; Kai *et al.*, 2021). Furthermore, the study by Kai (2018) identified that the December to May (DM) cyclone season is sub-divided in two sub-seasons; namely the December to February (DJF) wet sub-season, and the three wet months (March to May (MAM) sub-season. The two sub-seasons coincide with the DJFM TC and Tropical Storms (TS) peak season with a mean TC and TS frequency of 2.2 and 4.8 per season (Kai, 2018). The TCs not only influence the DJF and MAM (tending to enhance the rainfall during the two sub-seasons), but also have considerable influence on riverbank changes (erosion or accretion). The TCs influence on shorelines is mainly through the strong winds and waves which often accompany the TC events. When such waves collide with the shoreline they may head into the estuary and accelerate sediment erosion/deposition of the riverbanks. They may also give rise to longshore sediment transport, with localized areas of preferential shoreline accretion (Shaghude *et al.*, 2015).

Other studies show that TCs may also be associated with sporadic incidences of sea level rise or coastal inundations (flooding) of low-lying coastal areas (Yanxia *et al.,* 2013; Jonathan et *al.,* 2013; Larcombe and Carter, 2004).

An anecdotal survey of various age groups of people residing in the Rufiji Delta consistently agreed with the results presented above. The interviewed residents of the Rufiji Delta reported that most environmental changes (sediment deposition and erosion in the Delta and the Delta distributary channels) occur during December to April. The residents of Simbauranga acknowledged that their village has been facing considerable environmental degradation over time under the influence of strong waves and winds and most of the degradation occurs during the DJFM period. They further revealed that during the last 10 to 15 years, their shoreline had transgressed (moved landward) for an estimated distance of about 150 - 200 m (from current position) seaward (based on GPS measurements). Regeneration of new mangrove trees due to sediment deposition along the riverbanks, shifting of the distributary channels and erosion of the riverbanks were among the issues that were reported during the anecdotal survey.

The main challenge encountered during this study was acquisition of at least 95 % cloud free Landsat satellite imageries that also matched with the low tidal phase and the DJFM tropical cyclone season. Future studies with a similar objective should therefore consider employing microwave remote sensing sensors which are not affected by clouds.

It has been demonstrated in this study that TCs affect the Rufiji River estuary, delta and shoreline, on both a short-term and long-term basis. This work has indicated that regular monitoring of these critical habitats in other parts of the Tanzanian coast through oceanographic studies using remotely-sensed satellite data is possible, and is necessary to inform coastal planning and management efforts.

References

Bengtsson L (2007) Tropical cyclones in a warmer climate. World Meteorological Organization (WMO) Bulletin 56 (3):196-203

Boak EH, Turner, IL (2005) Shoreline definition and detection: A review. Journal of Coastal Research 21: 688 - 703

Camargo SJ (2013) Global and regional aspects of tropical cyclone activity in the CMIP5 models. Journal of Climatology 26: 9880-9902 [doi: 10.1175/jcli-d-12-00549.1]

Chang-Seng DS, Jury MR (2010) Tropical cyclones in the SW Indian Ocean. Part 1-Inter annual variability and statistical prediction. Meteorology Atmospheric Physics 106: 149-162

Chinsu L, Wu CC, Tsogt K, Ouyang YC, Chang CI (2015) Effects of atmospheric correction and pansharpening on LULC classification accuracy using WorldView-2 Imagery. Information Processing in Agriculture 2: 25-36

Charrua AB, Padmanaban R, Cabral P, Bandeira S, Romeiras MM (2021) Impacts of the Tropical Cyclone Idai in Mozambique: A multi-temporal Landsat satellite imagery analysis. Remote Sensing 13 (201) [doi.org/10.3390/ rs13020201]

Cooper MJP, Beevers MD, Oppenheimer M (2008) The potential impacts of sea level rise on the coastal region of New Jersey, USA. Climate Change 90: 475 -492

Dolan R, Fenster MS, Holme, SJ (1980) Temporal analysis of shoreline recession and accretion. Journal of Coastal Research 7 (3): 723-744

Doody K, Hamerlynck O (2003) Biodiversity of Rufiji District – A summary environmental management and biodiversity conservation of forests, woodlands, and wetlands of the Rufiji Delta and floodplain. REMP Technical Report 44: Biodiversity Summary. 101 pp

Erftemeijert PLA, Hamerlynck, O (2005) Die-back of the mangrove Heritiera Southeast Queensland, Australia. Estuarine Coastal and Shelf Science 85: 292-298

FAO (1960) The Rufiji basin, Tanganyika. FAO report to the government of Tanganyika on the preliminary reconnaissance survey of the Rufiji basin. Volume ii. Hydrology and water resources, Part (i). Computation and analyses. 405 pp

Fisher JS, Overton MF (1994) Interpretation of shoreline position from aerial photographs. International Conference on Coastal Engineering. Kobe, Japan. pp 1998–2003

Fisher PR, Dyer K, Semesi A (1994) Rufiji delta hydrodynamics research program, Final report: Characteristic circulation and sedimentation in the Rufiji delta, Tanzania. Frontier-Tanzania Technical Report No. 13. The Society for Environment Exploration, UK. 295 pp

Francis J (1992) Physical processes in the Rufiji delta and their possible implications on the mangrove ecosystem. Hydrobiologia 247: 173-179

Frouin R, Schwindling M, Deschamps PY (1996) Spectral reflectance of sea foam in the visible and near infrared: *In situ* measurements and remote sensing implications, Geophysical Research 101: 14361-14371

Holland GJ (1993) The global guide to tropical cyclone forecasting. World Meteorological Organization, Geneva. 337 pp

Hafslund AS (1980) Stiegler's Gorge power and flood control development. Project Planning Report, Vol. 1. Consultant Report submitted to RUBADA.

Jensen JR (1996) Introductory digital image processing (2nd edition). Upper Saddle River, NJ. Prentice Hall. pp 184 and 318

Jonathan D, Woodruff I, Jennifer LI, Camargo SJ (2013) Coastal flooding by tropical cyclones and sea-level rise. Nature 504: 44-52

Kai KH (2018) Impacts of Southwestern Indian Ocean tropical cyclones and storms on the rainfall pattern and vegetation productivity over Tanzania. PhD thesis, Institute of Marine Sciences, University of Dar Es Salaam, Dar Es Salaam. 279 pp

Kai KH, Ngwali MK, Faki MM (2021) Assessment of the impacts of Tropical Cyclone Fantala to Tanzania coastal line: Case study of Zanzibar. Atmospheric and Climate Sciences 11: 245-266 [https://doi.org/10.4236/acs.2021.112015]

Larcombe P, Carter R (2004) Cyclone pumping, sediment partitioning and the development of the Great Barrier Reef shelf system. Quarterly Scientific Review 23: 107-135

Lohani B, Mason, DC (1999) Construction of a digital elevation model of the Holdness Coast using the waterline method and Airborne Thematic Mapper data. International Journal of Remote Sensing 20: 593-607

Mavume AF, Rydberg L, Mathieu R, Johann R, Lutjeharms E (2006) Climatology and landfall of tropical cyclones in the South West Indian Ocean. Western Indian Ocean Journal of Marine Sciences 8 (1):15-35

Monga E, Mangora MW, Mayunga JS (2018) Mangrove cover change detection in the Rufiji Delta in Tanzania. Western Indian Ocean Journal of Marine Science 17 (2): 1-10

Muzuka ANN, Shaghude YW (2000) Grain size distribution along the Msasani beach, north of Dar es Salaam harbour. Journal of African Earth Sciences 30 (2): 417 – 426 [Doi: 10.1016/S0899-5362(00)00027-0]

Muzuka ANN (2001) Sources of organic matter in the Msasani bay and Dar es Salaam harbour. In: Richmond MD, Francis J (eds) Marine science development in Tanzania and Eastern Africa. Proceedings of the 20th Anniversary Conference on Advances in Marine Science in Tanzania, 28 June-1 July 1999, Zanzibar, Tanzania. IMS/WIOMSA. pp 51-60

Nayak SR (2002) Use of satellite data in coastal mapping. Indian Cartographer: 147-157

Nyandwi N (2001) Reassessment of the nature of beach erosion north of Dar *es* Salaam, Tanzania. In: Richmond MD, Francis J (eds) Marine science development in Tanzania and Eastern Africa. Proceedings of the 20th Anniversary Conference on Advances in Marine Science in Tanzania, 28 June-1 July 1999, Zanzibar, Tanzania. IMS/WIOMSA. pp 107-120

Ndesanjo R, Ngana JO, Yanda PZ (2012) Climate change impact and adaptive strategies in the Rufiji Delta, Tanzania. UTAFITI 9 (1&2): 57-73

Pardo-Pascual JE, Almonacid-Caballer J, Ruiz LA, Palomar-Vázquez J (2012) Automatic extraction of shorelines from Landsat TM and ETM+ multi-temporal images with sub pixel precision. Remote Sensing of Environment 123: 1-11

Pugh D (1996) Tides, surges and mean sea level. John Wiley & Sons, Chichester, UK. 472 pp

Pugh D (2004) Changing sea levels: Effects of tides, weather and climate. Cambridge University Press. 280 pp

Punwong P (2013) Holocene mangrove dynamics and sea level changes: records from the Tanzanian coast. PhD Thesis, University of York. 295 pp

Richmond MD, Wilson JDK, Mgaya YD, LeVay L (2002) Analysis of small-holder opportunities in fisheries, coastal and related enterprises in the floodplain and delta areas of Rufiji River, Tanzania. Rufiji Environment Management Project. Technical Report 25 [http: //coastalforests. tfcg.org]

RUBADA (2001) Development of Stiegler's Gorge multipurpose project for hydropower, agriculture and flood control. Rufiji Basin Development Authority RUBADA.

Semesi AK (1992) Developing management plans for the mangrove forest reserves of mainland Tanzania. Hydrobiologia 247: 1-10

Shaghude YW, Wannäs KO, Lunden B (2003) Assessment of shoreline changes in the western side of Zanzibar channel using satellite remote sensing. International Journal of Remote Sensing. 24 (23): 4955-4969

Shaghude YW (2004) Coastal impacts of water abstraction and impoundment in Africa: The case of Rufiji River. Final report submitted to START, March 2004. 75 pp [OceanDocs: E-Repository of ocean publications, http://iodeweb1.vliz.be/odin/bitstream/1834/187/1coastal.pdf]

Shaghude YW, Nyandwi N, Muzuka ANN, Dubi AM, Mwaipopo OU (2006) Sediments characteristics and hydrodynamic settings of reef platform sediments of Kunduchi, north of Dar es Salaam harbour. Tanzania Journal of Science 32: 36-52

Shaghude YW, Dubi AM, Nyandwi N, Muzuka ANN, Shalli, M. Sanga I (2007) Report on the training course on shoreline changes, mitigation and monitoring to the DoE staff, Zanzibar. Report submitted to SMOLE, Zanzibar. 62 pp

Shaghude YW, Mburu JW, Arthurton RS, Dubi A, Gachuiri S, Kangwe J, Magori C, Msuya F, Mwaipopo R, Nyandwi N, Ochiewo J, Ong'anda H, Sallema RM,

Sanga I, Shalli M, Uku J (2015) Shoreline change in Tanzania and Kenya – A manual for assessment and design for mitigation strategies. WIOMSA Book Series No 16. WIOMSA, Zanzibar. pp xii + 85

Shaghude YW (2016) Estuarine environmental and socio-economic impacts associated with upland agricultural irrigation and hydropower developments: The case of Rufiji and Pangani Estuaries, Tanzania. Estuaries: A lifeline of ecosystem services in the Western Indian Ocean. Springer, Cham, Switzerland. pp 169–182 [doi.org/10.1007/978-3-319-25370-1_11]

Singh A (1989) Digital change detection technique using remotely sensed data. International Journal of Remote Sensing 10: 989-1003

Song C, Woodcock C, Seto K, Lenney MP, Macomber S (2001) Classification and change detection using Landsat TM data: When and how to correct atmospheric effects? Remote Sensing of Environment 75: 230-244

Timiza W (2011) Climate variability and satellite – observed vegetation responses in Tanzania. MSc Thesis in Physical Geography and Ecosystem Analysis, Lund University. Seminar series 205, 30 ECTS

Tsai F, Chen WW (2008) Striping noise detection and correction of remote sensing images. IEEE Transactions on Geoscience and Remote Sensing 46 (12). pp 4122-4131 [doi: 10.1109/TGRS.2008.2000646]

Williams GD, Thom RM (2001) Marine and estuarine shoreline modification issues. PNWD-3087. Prepared for Washington Department of Fish and Wildlife, Washington Department of Ecology and Washington State Department of Transportation by Battelle Marine Sciences Laboratory, Sequim, Washington

Williams GD, Thom RM, Miller MC, Woodraf DR, Evans NR, Best PN (2003) Bainbridge Island near shore ecosystem. Summary of best available sciences. PNWD 3233, Bainbridge Island. Battelle of Marine Sciences Laboratory. Sequim, WA. 250 pp

Yanxia L, Haijun H, Zhongfeng Q, Jianyong F (2013) Detecting coastline change from satellite images based on beach slope estimation in a tidal flat. International Journal of Applied Earth Observation and Geoinformation 23: 165-176